– : Morphologischer Atlas Lieferung I: Morphologie des Meßtischblattes Stadtremda. Mitt. Geogr. Ges. Hamburg 28, Hamburg 1914.

RATHJENS, C.: Morphologischer Atlas Lieferung II: Morphologie des Meßtischblattes Saalfeld. Hamburg 1920.

RICHTER, H.: Eine neue Methode der großmaßstäbigen Kartierung des Reliefs. In: Petermanns Geogr. Mitt. 106, 1962, S. 309-312.

SPÖNEMANN, J.: Morphographic Mapping in Different Scales: A System of Generalisation. In: Techn. Pap. 12th Conf. Int. Cartogr. Assoc., Perth, Australia 1984, Vol. 2, S. 491-504.

STÄBLEIN, G.: Die Konzeption der Geomorphologischen Karten GMK 25 und GMK 100 im DFG-Schwerpunktprogramm. In: Berliner Geogr. Abh. 31, Berlin 1980, S. 13-30.

VINKEN, R.: Digitale Geowissenschaftliche Kartenwerke – ein neues Schwerpunktprogramm der Deutschen Forschungsgemeinschaft. In: Nachr. Karten- u. Vermessungswesen RI 95, 1985, S. 163-173.

EVALUATION OF ALGORITHMS FOR MAPPING SNOW COVER PARAMETERS IN THE FEDERAL REPUBLIC OF GERMANY USING PASSIVE MICROWAVE DATA*

With 8 figures

AXEL J. SCHWEIGER and ROGER G. BARRY

Zusammenfassung: Bewertung von Methoden zur Schneeflächenkartierung in der Bundesrepublik Deutschland mit Hilfe passiver Mikrowellendaten.

Ziel der vorliegenden Studie ist die Bewertung der Anwendungsmöglichkeiten passiver Mikrowellen-Fernerkundungsmethoden für die Untersuchung mitteleuropäischer Schneeflächenvariabilität. Schneemächtigkeiten und Wassergehaltsmessungen von 60 synoptischen Stationen in der Bundesrepublik Deutschland wurden mit den Ergebnissen eines auf der Differenz der 37 und 18 GHz Kanäle von SMMR (Scanning Multichannel Microwave Radiometer) beruhenden Algorithmus verglichen. Die Ergebnisse zeigen, daß nach Anpassung von Algorithmus-Parametern die Schneebedeckung mit 70 bis 80-prozentiger Genauigkeit bestimmt werden kann. Die Anpassung des Diskriminationsschwellenwertes für bewaldete Gebiete führt zu einer Verbesserung der Meßgenauigkeit. Aufgrund großer Temperaturschwankungen und häufig nassen Schnees ist die Anwendung von passiven Mikrowellenmethoden für die Bestimmung des Schnee-Wassergehaltes in diesem Gebiet ungeeignet.

* This work has been supported by NSF grant SES-8518586. Image processing was facilitated through ONR URI grants N00014-87-G-0022 and N00014-85-C-0039. DMSP imagery was provided by GREG SCHARFEN, National Snow and Ice Data Center. SMMR Cell-All tapes were provided by P. GLOERSEN, NASA/Goddard Space Flight Center. Thanks are also due to Dr. L. HOFFMANN, Deutscher Wetterdienst, for providing digital snow data sets.

1. Introduction

Information on snow cover is of wide interest to climatologists and hydrologists on a global scale. Primarily, snow cover is recognized as a potentially important factor in climate fluctuations, through its effect on the surface and planetary albedo. For example, seasonal snow cover might play an important role in amplifying the effects of a global CO_2 induced warming by means of positive feedback effects (BARRY 1985). Though a 20 year global data set of weekly snow charts has been derived from visible band imagery (MATSON et al. 1986), its utility for climate change studies is limited by the inability of visible band based techniques to map snow in the presence of clouds (HALL 1988).

The retrieval of snow cover parameters from passive microwave satellite data has been developed over the past 10 years. These techniques are based on the relationship between snowpack properties and microwave emissions from the snow surface, (KUENZI et al. 1982, FOSTER et al. 1984). The advantage of passive microwave techniques over visible band and ground based measurements lies in their capacity to provide information on snow cover parameters such as snowline position, total snow extent, and approximate snow water equivalent, even in the presence of clouds. While the potential of passive microwave techniques for the study of snowcover-climate interactions is great, their validation so far has been limited to homogeneous areas with deep non-melting snow packs.

This study assesses the accuracy of passive microwave algorithms through a comparison with ground based measurements and snow cover data derived from visible band imagery for typical European conditions. Such conditions consist of the occurrence of frequent melt events during the snow season, the presence of forest vegetation, and diverse terrain types ranging from flat homogeneous terrain to "middle mountains" with elevations up to 1000 m. Areas displaying the greatest variability in snow cover extent and therefore climatologically of particular interest are located near the snowline, - the "snow transition" zone (KUKLA 1979) and experience frequent melt events during the snow season. Melting snow packs become impermeable for microwaves at frequencies of 37 GHz and 18 GHz (employed by current sensors) and pose a significant problem for the retrieval of snow cover parameters under such conditions.

2. *Data and data processing*

Early studies using heterogeneous data have shown a considerable spatial variability of the seasonal snow cover in central and northern Europe (DICKSON and POSEY 1967) but data sparsity has so far limited a more thorough study of the short and long term variability of European snow cover.

The Federal Republic of Germany was selected as a test area because it provides a diversity of enviromental conditions broadly representative of other central and northern European countries. Daily snow depth data based on ruler measurements at 60 synoptic stations were obtained from the German weather service (Deutscher Wetterdienst). The data were gridded to a UTM grid with a mesh width of 10 km and, using a computer contouring package, contour maps of daily snow depth were produced. For a quantitative comparison with data from the Scanning Multichannel Microwave Radiometer (SMMR), ground measurements were interpolated using a spatial filtering technique (ELIASON and SODERBLOM 1978). Microwave brightness temperatures at 37 GHz and 18 GHz, both vertical and horizontal polarizations, were extracted from the CELL ALL tapes and gridded to a UTM grid. Those two frequencies provide most information on snow cover parameters (KUENZI et al. 1982). Lower frequency channels, potentially useful for information on the state of the underlying ground, or in the presence of wet snow, have resolutions that preclude regional scale applications.

A simple gradient algorithm developed by KUENZI et al. (1982) that discriminates between snow covered and snow free areas based on the brightness temperature difference of the 18 GHz and 37 GHz channels at horizontal polarizations, was then applied to the brightness temperature data set and maps of snow extent based on a "gradient threshold" (37_h-18_h) of -2 K were produced. The SMMR sensor operated on alternate days only. Therefore, the entire area was covered by a SMMR swath only every sixth day, and almost no night-time imagery is available. Days when a SMMR swath only partially covered the area were excluded.

Vegetation data

The effect of vegetation on the microwave emission from snow covered areas has been noted by several authors (HALLIKAINEN 1984; HALL et al. 1982). Forest vegetation affects the microwave emissions from snow cover through scattering and absorption within the canopy.

Data at subresolution are desirable to evaluate the contributions related to specific vegetation types within one pixel. Due to the lack of a suitable landcover dataset the necessary information was obtained from a mosaic of Landsat MSS imagery that exists in the form of a wall poster (WESTERMANN VERLAG 1980). The mosaic is based on the visible band and near infrared channels of the Landsat MSS sensor, with the near infrared channel displayed in green to achieve a "semi natural" appearance. Forested areas were clearly distinguishable. Using a high resolution scanner this poster was digitized, registered to the UTM grid at 1 km resolution and the amount of forest cover and water (large lakes only, and coastal areas) were determined in SMMR grid cells. Fractional amounts for four other vegetation classes were also determined, but were found to be of no significant influence for the retrieval of snow cover parameters.

Terrain Data

Terrain inhomogeneity presents a particular problem for the application of passive microwave data, since the unrepresentativeness of ground measurements in such terrain complicates the development and validation of reliable algorithms. Digital elevation data were extracted from a 5 minute resolution global data set and used in the interpolation of ground based snow depth measurements.

3. Analysis

Preliminary comparisons of the snow cover distribution shown by the contoured ground measurements and the SMMR algorithm demonstrated reasonable overall agreement (SCHWEIGER et al. 1987). However, more detailed assessment reveals many discrepancies in snow extent on a daily time scale and significant problems with estimates of snow water equivalent.

Interpolation of station measurements taking account of elevation

The validation of passive microwave algorithms has previously focused mainly on lowland areas. Elevated terrain influences the distribution of snowfall because of lower temperatures at higher elevations, through orographic effects on accumulation and the effect of slope orientation on ablation. Relief in the FRG is sufficient to require a correction for elevation as the single most important influence on the distribution of snow cover. For the present study an automated interpolation method incorporating a correction for elevation was devised and applied to the data set. The method is based on the differential weighting of individual measurements in the interpolation with respect to their elevation. Weighting factors were established from the analysis of the elevation dependence of snow depth measurements in this area. While preliminary in its development, the elevation weighted interpolation procedure (SCHWEIGER 1987) seems capable of producing correlative snow data more appropriate for the validation of remote sensing techniques than data interpolated solely using a station distance weighting.

Gridded and interpolated snow depth data are compared with the results of the SMMR snow extent algorithm using a threshold of -2 K for the difference between the brightness temperatures of the horizontal polarizations of the 37 GHz and 18 GH_2 channels (GR_h). Pixels below this threshold are classified as snow covered, pixels with greater values are snow free. For the classification based on ground data a threshold of 5 cm depth is used. Pixels with snow depth less than 5 cm were thus considered snow free.

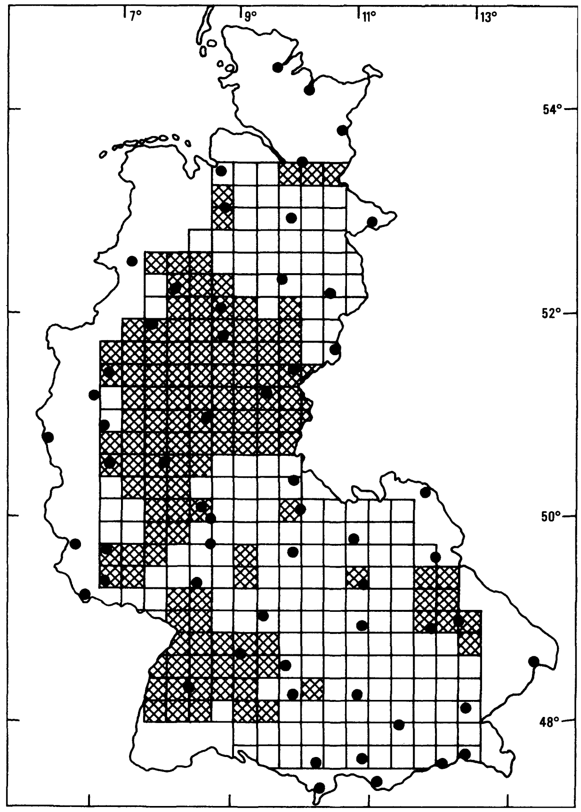

Fig. 1: Map of misclassified pixels for Jan 12 1979. Crosshatched areas indicate misclassified pixels
Karte der falsch klassifizierten Bildelemente für den 12. Januar 1979

Figure 1 shows pixels where there are disagreements between the SMMR algorithm and the ground data. The fairly large number of missclassified pixels is apparent. A comparison with meteorological data gives an explanation for this large number. Temperatures are above 0° and a storm with some rainfall had crossed Germany on the previous day. An increase in the liquid water content due to snow melt or rain results in a rapid increase in the brightness temperature gradient (GR_h), resulting in the classification of these pixels as snow free. Other cases are discussed in SCHWEIGER et al. (1987).

Time series analysis of brightness temperatures

The large variability in microwave emissions due to changes in snow pack parameters is apparent from time series of brightness temperatures, snow depth

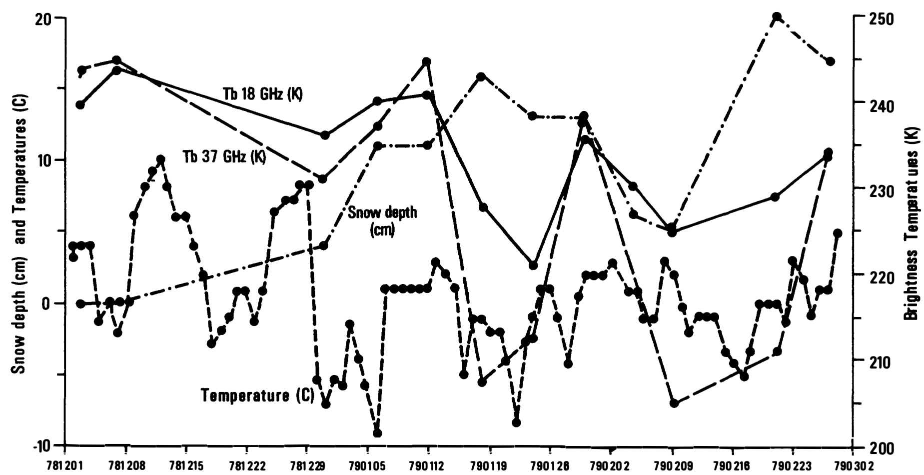

Fig. 2: Time series plot of snow depth, brightness temperatures and physical temperature for station Lingen. The station is located in northern Germany at an elevation of 21 m

Zeitreihe der Schneehöhe, Helligkeitswerte und Temperatur für die Station Lingen. Die Station liegt in Norddeutschland auf einer Meereshöhe von 21 m

measurements and physical temperatures for individual pixels.

The synoptic station Lingen is located in the north-western part of the FRG in flat terrain with little forest vegetation. The location provides a typical example of a lowland station in northern Germany. The time series plot for Lingen (Fig. 2) shows that the area is snow free until the last few days in 1978. Snow accumulation of 5 cm on Dec 29 1978 and Dec 30 1978 causes a drop in the brightness temperatures. Temperatures well below the freezing point cause the snow to be dry which is reflected in the development of the typical brightness temperature signature for snow covered areas, namely lower brightness temperatures in the 37 Ghz and 18 Ghz channel. Temperatures were above 0° C between Jan 6 1979 and Jan 12 1979 causing an increase in the liquid water content of the snow pack and resulting in the disappearance of the typical dry snow signature and a rise in the brightness temperatures. Snowfall in the beginning of the week between Jan 12 1979 and Jan 18 1979 increases the snow pack to 15 cm. Daily maximum temperatures below 0° C in the second half of this week cause a refreezing of the snow pack and a very sharp drop in the brightness temperatures. The magnitude of drop can hardly be explained by the temperature differences alone. The low brightness temperatures and the very low gradient, compared with the previous weeks could be explained by a growth in grain size related to diurnal melt freeze cycles. Maximum daily temperatures of only 2° C above freezing seem to generate sufficient melt to cause a sharp increase in brightness temperatures and a positive gradient in the week from Jan 24 1979 to Jan 30 1979 while the depth of the snow pack remains virtually constant. In spite of a decrease in snow depth to only 5 cm and mean daily temperatures above 0° C, freezing temperatures on Feb 5 1979 are sufficient to cause the redevelopment of a negative gradient. An increase in snow depth by 15 cm in the period until Feb 21 1979 surprisingly has no effect on the brightness temperatures pointing to the frequently wet nature of freshly fallen snow in this area.

At elevated stations in the German "Mittelgebirge" the effect of the terrain weighted interpolation algorithm is clearly visible. The time series plot for Kahler Asten (839 m elevation) in a middle mountain area with snow depths of up to 75 cm displays rather small changes in brightness temperatures compared to the enormous changes in snow depth (Fig. 3). This discrepancy is somewhat smaller when terrain corrected snow depths with a reduced variability are used for the comparison with the brightness temperatures. To a greater degree than in the previous example, brightness temperature changes seem to be influenced by the variability of snow pack parameters other than snow depth. Apart from the lack of colinearity between snow depth and microwave emissions, due to obvious changes in grain sizes and liquid water content, possible effects caused by the generally small snow depth and the considerable relief in the overall study area need to be considered.

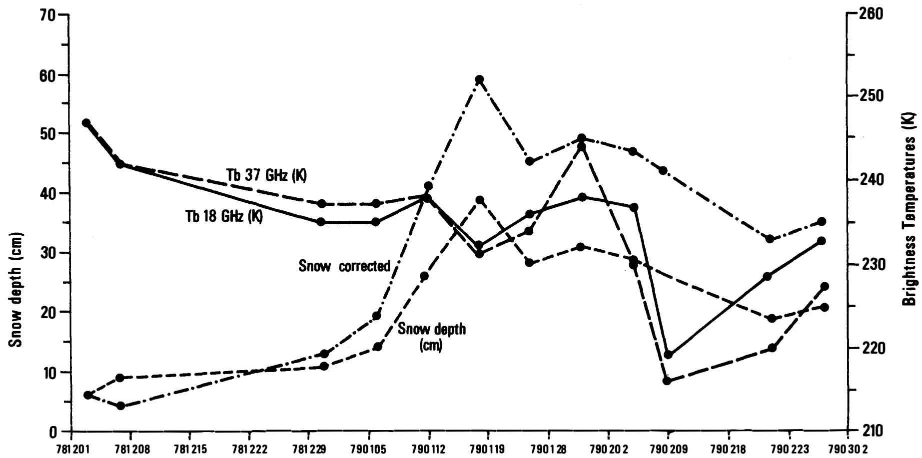

Fig. 3: Time series plot of snow depth and brightness temperatures for station Kahler Asten at an elevation of 839 meters

Zeitreihe der Schneehöhe und Helligkeitswerte für die Station Kahler Asten auf einer Meereshöhe von 839 m

The DMSP image in Figure 4 for Feb 21 1979 clearly shows that, despite a thick snow cover in the middle mountains of Germany, large areas appear dark and obviously not snow covered on the satellite image. This is in part due to the abundance of coniferous trees at higher elevations, as well as the higher variability of the snow distribution due to the ruggedness of the terrain. Microwave emission from a pixel in a mountainous area therefore consist of contribution from snow free ground, vegetation and the snow covered surface. This may explain the reduced sensitivity to snow depth variations. Even though this problem is accentuated in irregular terrain, it also needs to be considered for the lowlands when the snow pack is shallow. The interpretation of the microwave emissions from such partially covered pixels is further complicated when the snow-free soils undergo transitions from wet unfrozen to frozen soils or vice versa.

Analysis of average brightness temperatures

It is obvious that good correlations between daily snow depth and microwave emissions from the snow pack for this area can hardly be expected. Even though the use of night time imagery would probably reduce the brightness temperature variability somewhat by eliminating some of the effects due to daytime melt, the retrieval of water equivalent with the sufficient accuracy for research or practical application does not currently seem possible for Germany, or similar mid-latitude maritime climates.

Further investigation of the snow depth-microwave dependence is still of interest since it can potentially improve the accuracy of snow extent algorithms. Because the relationship between daily snow depth and brightness temperatures is complex, averages of snow depth and brightness temperature gradient for both seasons have been calculated for each pixel. Figure 5 shows the relationship of average pixel brightness temperatures to average pixel snow depth for stations below 400 m. The averaging process reduces the variability due to factors such as grain size and liquid water content and a relationship between snow depth and brightness temperatures can be obtained. The regression equation is given as

$$GR_h = (D_c - 11)/-0.785 \qquad (1)$$

where: GR_h = brightness temperature gradient
D_c = snow depth (corrected)

The slope of the regression line is considerably less than the relationship utilized by CHANG et al. (1986) for mapping global snow cover. The averaged result includes many melt events when gradients (GR_h) approach 0 K, hence the response is lower than model predictions for dry snow condition.

Determination of snow extent

The distinction between snow free and snow covered ground is of major concern for large scale cli-

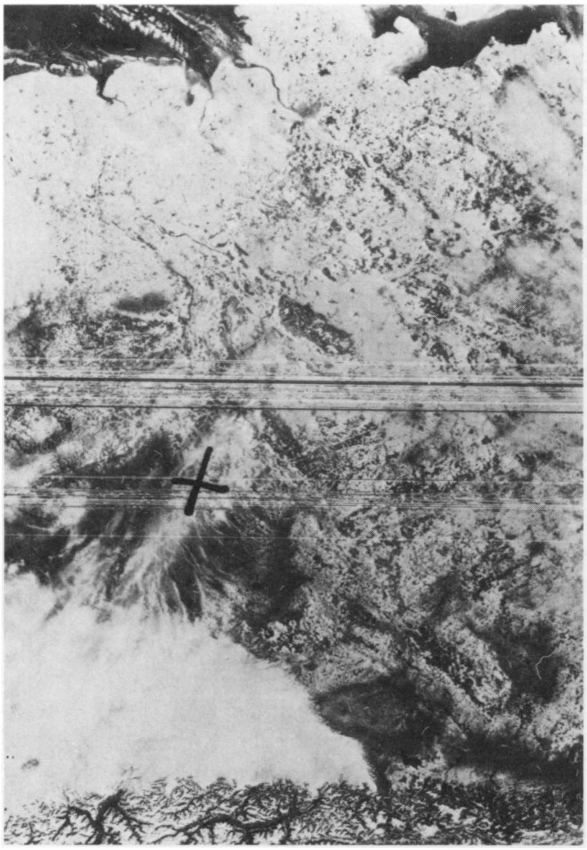

Fig. 4: DMSP visible band image for February 21 1979. Light tone area in the lower left part of the image is cloud covered

DMSP Satellitenbild (sichtbarer Bereich) für den 21. Februar 1979. Die linke untere Ecke weist Wolkenbedeckung auf

matological studies. KUENZI et al. (1982) found that a gradient threshold (GR_h) of −2 K gives the best match with continental or hemispheric snow extent shown by the NOAA/NESDIS snow chart whereas ROTT (1983) suggested a discrimination threshold of −5 K achieves the best fit for areas in central Asia. Figure 6 shows the histograms of the average pixel gradient values for cases when the snow depth exceeded 5 cm (left side) and snow free cases (right side). Gradient values for snow free areas show a maximum at 5 K. This relatively large positive brightness temperature gradient points to the fact that in the two winters investigated, the snow free ground was mostly wet and unfrozen. Average brightness temperature gradient values for snow covered pixels are mostly lower, thus allowing a discrimination between snow free and snow covered ground. KUENZI et al. (1982) employed a discrimination threshold of −2 K. From Fig. 6 it is obvious that a higher discrimination threshold of 0–2 K would provide a better discrimination. This discrepancy is due to the fact that frequent melt occurrences raise the average brightness temperature gradients of snow covered land, while at the same time greater GR_h values of snow free ground can be expected because of soil wetness. Using a discrimination threshold of 0 for the SMMR data produced the best classification results, when compared with ground data, using a 5 cm snow/no snow threshold. 75% of all pixels were correctly classified and a Chi-square test showed the results to be significant at the 0.001 level.

4. *Vegetation effects*

Emitted radiation from snow covered surfaces is modified by the vegetation cover through scattering and absorption within the canopy. For lack of an exact physical understanding of the radiative processes within the canopy, studies investigating the

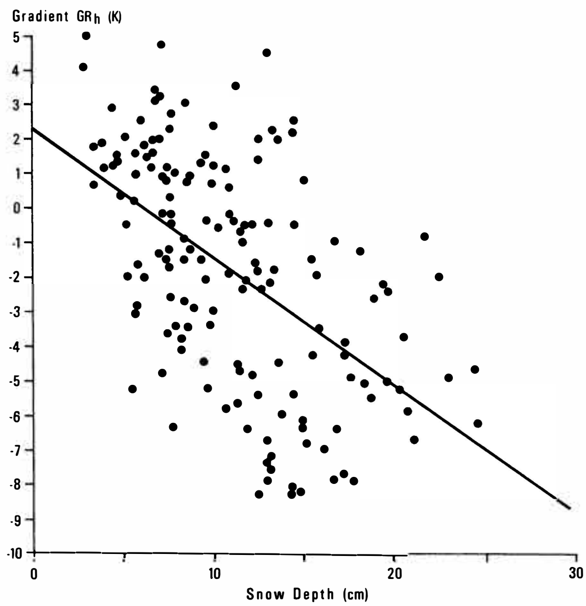

Fig. 5: Average gradient (GR_h) response to snow depth (elevation weighted interpolation) for stations below 400 meters. Both seasons were combined

Veränderung des Gradienten-Mittelwertes (GR_h) mit wachsender Schneehöhe (reliefbezogene Interpolation) für Stationen unterhalb 400 m Meereshöhe. Daten beider Winter zusammengefaßt

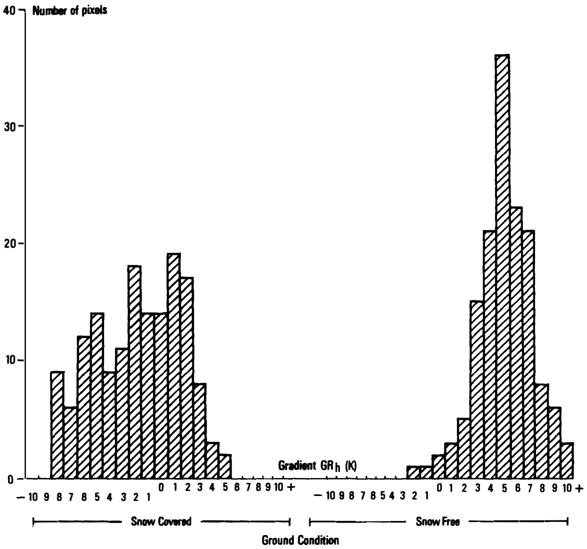

Fig. 6: Histograms of average pixel brightness temperature gradients (GR_h) for snow free and snow covered conditions

Histogramm der mittleren Gradientwerte (GR_h) für schneelose und schneebedeckte Bildelemente

effect of forest cover on the retrieval of snow cover parameters have so far been empirical. Results suggest there is an increase in brightness temperatures due to the high emissivity of vegetation (BURKE et al. 1984), and a decreased sensitivity of brightness temperatures to changes in snow pack parameters in forested areas (HALLIKAINEN et al. 1984).

Effects of vegetation in study area

Brightness temperatures over snow-free ground are found to be high and show little dependence on vegetation type. This result is quite surprising considering that soil moisture contents should vary considerably with vegetation type. Furthermore, lower brightness temperatures should be expected at 18_h GHz in forested areas due to the greater penetration depth at this frequency and the typically lower temperatures within the canopy near the surface. This suggests that the penetration depth differences are not substantial enough to produce a 37_h-18_h GHz brightness temperature gradient for canopy effects during the snow free part for the year.

Since vegetative cover has little effect on the microwave signature for snow free ground, the question arises whether vegetation over snow covered ground significantly modifies the brightness temperatures. As outlined above, the day-to-day brightness temperature variability due to changes in liquid water content, crystal grain sizes and areal snow distribution at sub-pixel resolutions is too large to allow any conclusions about canopy effects. To reduce this variability, mean brightness temperatures for all pixels have been calculated using observations from both seasons when the snow depth was greater than 5 cm. Pixels that are close to the coasts of the North Sea and Baltic Sea, as well as pixels in the vicinity of larger lakes are excluded from the analysis. Figure 7 shows the regression of average GR_h values on the amount of forest cover for both snow seasons combined. Average brightness temperatures for snow covered pixels are 5–30 K lower than for snow free conditions. Though correlations are weak, there seems to be a slight increase in average brightness temperatures with increasing forest cover within a pixel. The effect is not as strong as expected. The modest correlation may be due in part to the limited data sample. Brightness temperature gradient (GR_h), which is commonly used as an indicator of changes in snow pack conditions, shows no dependence on the amount of forested area. The majority of average pixel gradient values range between −1 and +4 K. These values are substantially higher than gradient values between 0.75 and −1.75 K observed by KUENZI et al. (1982).

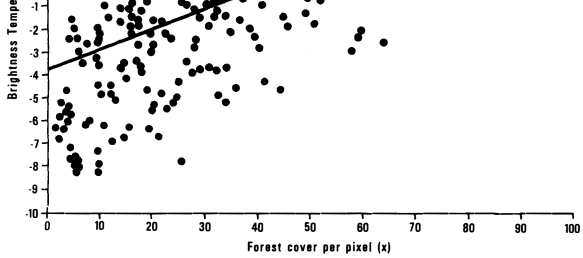

Fig. 7: Brightness temperature gradient (GR_h) with amount of forest cover during both seasons when snow depth on the ground was greater than 5 cm

Veränderung des Gradientwertes (GR_h) mit wachsender Waldbedeckung pro Bildelement. Daten für beide Winter wurden zusammengefaßt, wenn die Schneehöhe 5 cm übertraf

To investigate the relationship between forest cover, snow depth and brightness temperature gradients, a multiple linear regression analysis was performed on the average gradient values for each pixel, with snow depth and fractional amount of individual vegetation classes as independent variables.

$$GR_h = a + b_1 d + b_2 f_1 \quad (2)$$

where:

d = snow depth
f_1 = fractional amounts for each vegetation class
a = intercept
b_1, b_2 = regression coefficients

The best coefficients of determination were achieved for elevations below 400 m with about 50% explained variance, contributed almost equally by snow depth and forest cover. These results were obtained from average pixel values and therefore are not applicable for shorter term retrieval periods. However, they are encouraging in that they demonstrate the potential effect of vegetation on the accuracy of the snow cover parameter retrieval algorithm.

A conceptual problem arises from using a linear regression model, which assumes that the contributions of the snow cover and the vegetative cover are each linearly related to the gradient values and independent from one another. According to findings pertaining to soil moisture retrieval, the vegetation decreases the response to changes in surface properties. This means that a model should include variable responses for different vegetation classes. To assess this non-linearity a technique analogous to one developed by HALLIKAINEN et al. (1984) is used to describe the data by the following model.

$$GR_h = (f - 1)(TB_1 + a_1 d) + f(TB_2 + a_2 d) \quad (3)$$

where:

f = fractional amount of forest cover
$TB 1$ = gradient temperature for unforested snow free ground.
$TB 2$ = gradient temperature for forested snow free ground.
a_1 = specific response to snow depth for unforested areas.
a_2 = specific response to snow depth for forested areas.
d = snow depth.

The model explains 72% of the variance in the data if elevations above 500 meters are excluded. The confidence limits in the individual coefficients are still quite large. This fit was performed on average pixel values. An unexpected small positive value of a_2 for the specific response of forested areas indicates that the effect of snow depth on the brightness temperatures in forested areas is insignificant and that trees mask, rather than modify, response to snow cover. This also explains why a multiple linear regression model fits the data reasonably well. For this particular area, depth of snow packs under forest cover cannot be retrieved. This conclusion differs from the findings by HALLIKAINEN (1984) and HALL et al. (1983).

Influence of vegetation on snow extent retrieval

Several approaches can be taken to obtain optimum decision boundaries for gradient-based snow extent algorithms. Due to the limited reliability of the derived empirical equations 1 and 2 for a threshold snow depth of 5 cm, an optimum threshold was found through minimization of the classification error. To eliminate the possibility of chance results due to an uneven number of pixels for each class in the data set, the data set is subsampled on a random basis; thus the number of snow covered and snow free cases for each pixel is equal. Percentages of correctly classified days for each pixel are then calculated using a range of thresholds from −3 K to 6 K. Average percentages of correctly classified days for individual thresholds are grouped into 5 classes of fractional amount of forest cover as shown in figure 8. The proportion of correctly classified pixels clearly decreases with increasing amounts of forest cover per pixel. Also, pixels with less than 40% forest tend to display better classification results for higher threshold temperatures. Generally, the sensitivity to changes in threshold is smaller than expected; this is due to the errors introduced by factors such as excessive melt or unrepresentative station reports.

For each forest cover class, the threshold that produced the smallest number of misclassifications is then applied to the complete data set (for an equal number of snow covered and snow free pixels). The percentage of correctly classified pixels increases from 70 to 75%, compared with a fixed −2 K threshold suggested by KUENZI et al. (1982), but increases negligibly if compared with a constant threshold of 0 K. These values are rather low considering a chance probability of 50% for two classes. ROTT et al. (1983) report a substantially greater accuracy (75% to 95%) from a comparison of SMMR-derived snow extent and that given by the hemispherical NOAA/

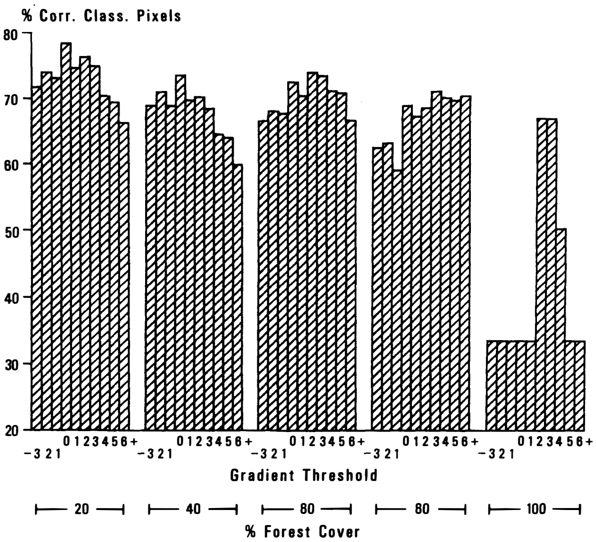

Fig. 8: Percent correctly classified pixels for 5 classes with different amount of forest cover per pixel. The histograms show the number of correctly classified pixels in percent for each threshold from - 3 to + 6. Note that for classes with greater amounts of forest cover higher thresholds result in greater percentages of correctly classified pixels

Prozentualer Anteil richtig klassifizierter Bildelemente in fünf Klassen unterschiedlicher Waldbedeckung pro Bildelement. Die Histogramme stellen die Anteile der richtig klassifizierten Bildelemente in Prozent für jeden Schwellenwert zwischen - 3 und + 6 dar. Für Klassen mit größerem Waldbedeckungsanteil führen höhere Schwellenwerte zu einer größeren Anzahl richtig klassifizierter Bildelemente

NESDIS snow charts using five day average minimum gradients. Considering that in this study only day time imagery was used, no time averaging was applied, and the area is located in a mid-latitude zone with frequent melt events, our result can be considered reasonable. The small improvement obtained when using variable thresholds has to be seen in light of the fact that areas with forest amounts exceeding 40% represent only a small fraction of the total area and are frequently located at higher elevations where the station data provide a poor correlative data base. The effect of forest cover on optimum gradient thresholds for snow mapping using minimum temperature gradients remains to be investigated since the vertical temperature structure within the canopy can be different at night. Due to the different penetration depths of the 18 and 37 GHz channels, GR_h values at night display different responses compared with day time data.

5. *Discussion and Conclusion*

Passive microwave snow cover algorithms have been tested for a mid-latitude area, where large temperature fluctuations during the snow seasons can lead to complications in the retrieval of snow cover parameters. While a reasonable match in the overall patterns of snow distribution is found between snow extent in the Federal Republic of Germany derived from SMMR data and interpolated snow depth measurements for 60 synoptic stations, considerable complications related to frequent melt events and the inhomogeneity of snow pack properties were encountered. As a result of higher temperatures in a mid-latitude climate, snow free soils are mostly unfrozen and wet during the winter season and display larger brightness temperature gradients (GR_h) than the dry and frozen soils in more northern regions. Snow packs in mid-latitude areas also show greater brightness temperature gradients due to a greater liquid water content caused by rain or melt.

The selection of a higher gradient threshold (GR_h = K) compared to the threshold of -2 K adopted for hemispheric snow mapping by other researchers increases the accuracy of retrieval by 5%. The average retrieval accuracy of 75%-80% of pixels (depending on amount of forest cover within a pixel) correctly classified pixels when compared to interpolated snow depth measurements (5 cm threshold) is lower than the accuracy at hemispheric scales, but seems reasonable in light of the incompatibilities between ground station data and satellite derived snow extent. These incompatibilities can be reduced if the interpolation of ground measurements is corrected for elevation effects using a digital elevation model and empirically derived climatological relationships between elevation, mean snow depth for the entire area on a given date, and the snow depth measured at an individual station.

Forest vegetation increases the brightness temperatures and masks gradient changes due to snow cover parameters. No snow cover information can therefore be retrieved from beneath a forest canopy. The results suggest that higher discrimination thresholds (+ 2) are appropriate for pixels with substantial amounts of forest cover. An increase in polarization ratios has been found with increasing snow depth. This effect has received little mention in the literature and points to the inhomogeneous stratigraphy of the snow cover in this area. Snow crust and ice lenses formed during melt freeze cycles have a major effect in reducing the horizontally polarized emissions and thereby cause an increase in the polarization ratios.

In summary, passive microwave techniques are capable of producing snow extent data sets for synoptic scale climate research in mid-latitude areas. Their ease of application in an automated fashion and the capability of mapping snow extent in the presence of persistent cloud cover constitutes the superiority of passive microwave techniques over current operational snow mapping procedures using visible band imagery, despite the greater accuracy of visible band techniques in the absence of cloud cover. The retrieval snow depth or water equivalent does not seem feasible for a mid-latitude area subject to winter melt events.

The results of this study suggest that gradient thresholds be adjusted with respect to temperature regime and forest cover in the areas of marginal snow cover. More research is needed to identify such regions with respect to their temperature and precipitation regimes in a spatial and temporal sense.

Passive microwave data from the SSM/I sensor launched in mid 1987 will provide a better coverage, with nighttime imagery, as well as information in the 85 GHz band, at a 12.5 km resolution (Weaver et al. 1987). The utility of this channel for the retrieval of snow parameters still needs to be investigated, but ground based measurements indicate its potential to allow a better discrimination of wet from dry or frozen land.

References

Barry, R.G: Snow cover, sea ice and permafrost. In: *Department of Energy:* Glaciers, Ice Sheets, and Sea Level: Effect of a CO_2 induced Climatic Change. Washington D. C. 1985, 241-247.

Burke, H. K., Bowley, C. F. and Barnes, C.: Determination of snow pack properties from satellite passive microwave measurements. In: Remote Sensing of the Enviroment 15, 1984, 1-20.

Chang, A. T. C., Foster, J. L. and Hall, D. K.: Nimbus 7 SMMR derived global snow cover parameters. In: Annals of Glaciology 9, 1986, 39-44.

Dickson, R. R. and Posey, J.: Maps of snow cover probability for the northern hemisphere. In: Monthly Weather Review 95 (6), 1967, 374-383.

Eliason, E. M. and Soderblom, L. A.: An array processing system for lunar geochemical and geophysical data. In: Proceedings of the 8th Lunar Science Conference 1978, 1163-1170.

Foster, J. L., Hall, D. K. and Chang, A. T. C.: An overview of passive microwave snow research and results. In: Reviews of Geophysics and Space Physics 22 (2), 1984, 195-208.

Hall, D. K.: Assessment of polar climate change using satellite technology. In: Reviews of Geophysics and Space Physics 26 (1), 1988, 26-39

Hall, D. K., Foster, J. L. and Chang, A. T. C.: Measurement of microwave emission from forested snow fields in Michigan. In: Nordic Hydrology 13, 1982, 129-138.

Hallikainen, M. T.: Retrieval of snow water equivalent from Nimbus 7 SMMR data: effect of land cover categories and weather conditions. In: IEEE Journal of Oceanic Engineering OE 9 (5), 1984, 372-376.

Kuenzi, K. F., Patil, S. and Rott, H.: Snow cover parameter retrieved from Nimbus 7 SMMR data. In: IEEE Transactions on Geosciences and Remote Sensing GE 20, 1982, 452-467.

Kukla, G. J.: Climatic role of snow covers. In: Allison, I. (ed.): Sea level Ice and Climate Change. Publication No. 131, International Association of Hydrological Sciences. Wallingford, Oxford 1979, 79-108.

Matson, M., Ropelewski, C. F. and Varnadore, M. S.: An atlas of satellite-derived northern hemisphere snow cover frequency. NOAA/NESDIS/NWS 1986, 74pp.

Rott, H. and Kuenzi, K.: Properties of the global snow cover and of snow free terrain from the Nimbus 7 SMMR first year data set. In: Proceedings of the specialist meeting on microwave radiometry and remote sensing application (Rome, March 1983) 1983, 7-18.

Schweiger, A. J., Armstrong, R. and Barry, R. G.: Snow cover parameter retrieval from various data sources in the Federal Republic of Germany. In: Goodison, B., Barry, R. G. and Dozier, J. (eds.): Large scale effects of seasonal snow cover. Publication No. 166, International Association of Hydrological Sciences. Wallingford, Oxford 1987, 353-364.

Weaver, R. L., Morris, C. and Barry, R. G.: Passive microwave data for snow and ice research: planned products from the DMSP SSM/1 System, EOS, 68 (39), 769, 776-777.

Westermann Verlag: Satellitenbildkarte Bundesrepublik Deutschland. Braunschweig 1980.